Ultrastructural Characterization of Gerbil Olivocochlear Neurons Based on Differential Uptake of 3H-D-Aspartic Acid and a Wheatgerm Agglutinin-Horseradish Peroxidase Conjugate from the Cochlea

Robert H. Helfert,[1,2] Ilsa R. Schwartz,[2,a] and Allen F. Ryan[3]

[1]Department of Anatomy and [2]Division of Head and Neck Surgery, UCLA School of Medicine, Los Angeles, California 90024, and [3]Division of Otolaryngology, Veterans Administration Medical Center and UCSD School of Medicine, La Jolla, California 92093

Two populations of olivocochlear (OC) neurons have been identified in the gerbil brain stem on the basis of differential labeling patterns of 3H-D-aspartic acid (D-ASP) and wheatgerm agglutinin–horseradish peroxidase conjugate (WGA/ HRP) from the cochlear perilymph. While both populations are capable of uptake and retrograde uptake of WGA/HRP, one population accumulates and retrogradely transports D-ASP (D-ASP OC neurons) and the other does not (non-D-ASP OC neurons).

D-ASP OC neurons are found in or near the lateral superior olive, are small in size, and receive very few synaptic contacts. The vast majority of these synapses contain small, mildly pleomorphic vesicles with scattered dense core vesicles. Synapses with distinctly larger pleomorphic vesicles have also been observed. These neurons possess all of the features common to neurons of the lateral olivocochlear system.

Non-D-ASP OC neurons are found primarily in the ventral nucleus of the trapezoid body, as well as in the area between the medial superior olive and the medial nucleus of the trapezoid body. These neurons are larger and receive greater numbers and types of synaptic contacts than those found on D-ASP OC neurons. The 2 most common synapses found on non-D-ASP OC neurons are axosomatic ones containing small, mildly pleomorphic vesicles and scattered dense core vesicles similar to those seen on the D-ASP OC neurons, and axodendritic synapses containing large, round vesicles. Much less frequently observed are synapses containing small, round vesicles or ones containing predominantly flat vesicles. The ultrastructural features of the non-D-ASP OC neurons correspond to those described for neurons of the medial olivocochlear system.

The population of superior olivary complex neurons that provides efferent innervation to the hair cells of the organ of Corti, the olivocochlear system, has been divided into lateral and medial components by Warr (1975, 1978) and his colleagues (Warr and Guinan, 1979; Warr et al., 1982, 1986; Adams, 1983; Guinan et al., 1983, 1984; White and Warr, 1983). This characterization resulted from studies using the cat as the experimental model. Similar correlations have been made in both New and Old World monkeys (Strominger et al., 1981; Thompson et al., 1984) and in a variety of rodent models such as rat (White and Warr, 1983; Osen et al., 1984), mouse and chinchilla (Osen et al., 1984), guinea pig (Fex and Altschuler, 1981; Fex et al., 1982a; Strutz and Bielenberg, 1983; Thompson et al., 1984), and gerbil (Schwartz and Ryan, 1986; Ryan et al., 1987). This division was based on the differences between the neurons of the 2 groups in the morphology and distribution, in the laterality of their efferent projections, and in their innervation patterns within the cochlea. The small, lateral olivocochlear (LOC) neurons are located within, or in the immediate vicinity of, the lateral superior olive (LSO), and most project to the ipsilateral cochlea and terminate beneath the inner hair cells. More specifically, they contact the afferent dendrites of type 1 spiral ganglion cells receiving input from the inner hair cells (Liberman, 1980; Schwartz and Ryan, 1986). Most medial olivocochlear (MOC) neurons are located medial and rostral to the LSO; the majority of these neurons project to the contralateral cochlea and the remainder innervate the ipsilateral cochlea. The efferent endings of the medial system terminate directly on the outer hair cells and may also be the source of additional efferent innervation to the dendrites of the type 1 neurons beneath the inner hair cells (Schwartz and Ryan, 1986; White et al., 1986).

Both direct and indirect evidence indicate that most, if not all, LOC neurons possess unmyelinated axons (Rasmussen, 1960; Fex and Altschuler, 1981; Arnesen and Osen, 1984; Ryan et al., 1987) and that the axons of MOC neurons are myelinated (Rasmussen, 1946; Fex et al., 1982a). While olivocochlear (OC) neurons in general appear to be cholinergic (Osen and Roth, 1969; Bobbin and Konishi, 1971; Jasser and Guth, 1973; Warr, 1975; Fex et al., 1982b; Osen et al., 1984), several biochemical distinctions have been made between neurons of the LOC and MOC systems. Immunohistochemical studies show that LOC perikarya label with antibodies to tyrosine hydroxylase (Altschuler et al., 1986a), calcitonin gene-related peptide (Schweitzer et al., 1985; Adams, 1986), met-enkephalin (Fex and Altschuler, 1981; Altschuler et al., 1983, 1984a; Eybalin and Pujol,

1984), while MOC fibers label with antibodies to aspartate aminotransferase (Fex et al., 1982a). Uptake studies using radioactively labeled amino acids indicate that the LOC neurons preferentially accumulate and retrogradely transport D-aspartic acid (D-ASP) (Schwartz and Ryan, 1986; Ryan et al., 1987), and MOC neurons (along with a few LOC neurons outside the LSO) label by the retrograde transport of nipecotic acid, a GABA analog, from the cochlea (Ryan et al., 1986).

Our studies using acetylcholinesterase histochemistry (a presumptive marker for OC neurons) and retrograde transport of HRP from the cochlea (a definitive marker for OC neurons) have shown similar patterns of distribution of labeled cells in the gerbil superior olivary complex (Helfert and Schwartz, 1987). The distribution of OC neurons in the gerbil LSO parallels that of both the small neurons and class 5 neurons (Helfert and Schwartz, 1987), i.e., the LSO-related OC neurons are distributed mostly within the middle and medial limbs of the LSO, with fewer found in the lateral limb. These distribution patterns also agree with the ones described in the gerbil LSO for LOC neurons labeled by retrograde transport of tritiated D-ASP from the cochlea (Ryan et al., 1987). It is still unresolved whether the small neurons compose the entire population of "intra-LSO" OC neurons, as suggested by Ryan et al. (1987) or whether class 5 neurons also contribute to this population.

This study was undertaken to characterize the ultrastructure of the OC neurons residing in the gerbil lower auditory brain stem, noting differences between neurons of the LOC and MOC systems, as well as possible differences between neurons within each system. It uses the differential ability of the OC neuron to accumulate and retrogradely transport tritiated D-ASP from the cochlea to distinguish between the classes of OC neurons. Most, if not all, gerbil LOC neurons are labeled autoradiographically by selective retrograde transport of D-ASP from the cochlea, while the MOC neurons are incapable of such transport (Ryan et al., 1987). Whether or not a population of non-D-ASP-labeled LOC neurons exists within or near the LSO is still open to question. By perfusing the cochlea with a solution containing both WGA and D-ASP, D-ASP-preferring OC neurons will be double-labeled, while non-D-ASP-preferring OC neurons will be labeled by WGA only. As a result, details of the fine structure of these 2 groups of OC neurons can be appraised and compared. A preliminary report on some of these findings has appeared (Helfert et al., 1986).

Materials and Methods

Mongolian gerbils (*Meriones unguiculatus*) were obtained from Tumblebrook Farms (West Brookfield, MA) or bred at UCLA from animals derived from Tumblebrook Farms stock. Young "adult" animals, 30–60 d of age (25–65 gm), were selected to avoid the possible influences of age-related changes found in the cochlear nuclei of older animals (Morest et al., 1986; Ostapoff et al., 1987). While some aspects of development are still incomplete in gerbils from this age range, most physiological parameters of auditory function that have been measured in the lower auditory brain stem of this species have adult characteristics by 30 d of age (Ryan et al., 1982; Woolf and Ryan, 1985).

Six animals were anesthetized with pentobarbital (30 mg/kg) and ketamine (40 mg/kg), and the posterior bulla was surgically exposed and opened, accessing the cochlea. Small holes were hand-drilled into the scala tympani of the basal turn and into the vestibule dorsomedial to the oval window. Ten microliters of oxygenated artificial perilymph (Nuttall et al., 1977), containing 2% (wt/vol) wheat germ agglutinin conjugated to horseradish peroxidase (WGA/HRP) (Sigma L 9008), and 80 μCi D-[2,3-^{3}H]-aspartic acid (D-ASP) (New England Nuclear) were injected through the scala tympani hole, filling both the scala tympani and scala vestibuli. The egress of fluid was observed from the vestibule hole as cochlear perilymph was being displaced by the artificial peri-

lymph solution. This fluid was wicked away. The holes were then plugged with bone wax and the surgical field was closed.

After a 24 hr-survival period, the animals were perfused transcardially with 15 ml of 0.05% sodium nitrite in normal saline, followed by ~200 ml of 1.25% glutaraldehyde and 1.0% paraformaldehyde in 0.12 M phosphate buffer, pH 7.3. Following removal from the skulls and postfixation for 2–4 hr in the same fixative, the brain stems were rinsed for 4–12 hr in 0.12 M phosphate buffer (pH 7.3) embedded in 5% agar, and transverse sections were cut at 150 μm using an oscillating tissue slicer (Frederick Haer OTS 3000). These sections were reacted with diaminobenzidine using the HRP development techniques described by Itoh et al. (1979). They were then postfixed with 2% osmium tetroxide in 0.1 M cacodylate buffer, pH 7.3, stained *en bloc* with uranyl acetate (Karnovsky, 1967), dehydrated through a graded ethanol series and propylene oxide, and embedded in Epon–araldite resin.

For light-microscopic autoradiography, groups of 1 μm sections were cut from each plastic block on a Sorval MT2 ultramicrotome and mounted onto 4 glass slides. These slides were dipped in Kodak NTB-2 emulsion and then exposed for 7, 14, 28 d, and 6 month intervals, respectively. After exposure, the slides were developed in Kodak Dektol (2 min at 17°C), counterstained with 1% toluidine blue in 1% aqueous sodium tetraborate, and examined and photographed with a Nikon Optiphot. Some observations on the distribution of the labeled neurons from this material have been published (Ryan et al., 1987). After the labeled cells were identified light-microscopically, each block was trimmed to the area containing these cells, and 60–90 nm thin sections were cut and processed autoradiographically as described in Schwartz and Bok (1979). The sections were exposed for time periods of 3 weeks to 6 months, then developed, collected on grids, and examined with a Siemens Elmiskop 1A. The silver grains resulting from the decay of tritium were obvious in the D-ASP-labeled profiles; the peroxidase granules were more intensely electron opaque than the electron dense organelles normally seen in unlabeled cells. Both labels were confirmed light-microscopically from sections adjacent to those prepared for ultrastructural study. Every labeled profile was photographed and analyzed at a final magnification at 16,000×, and each synapse was studied at a final magnification of 50,000×.

Results

Two populations of OC neurons were identified in this study on the basis of their differential labeling patterns. One group of OC neurons labeled with both WGA/HRP and D-ASP, while the second group contained WGA/HRP alone; i.e., neurons belonging to the former group were capable of preferential uptake of D-ASP, and neurons of the latter group were not. The D-ASP-preferring OC neurons differ morphologically from their non-D-ASP-preferring counterparts in size, in the composition of their synaptic input, and, to some extent, in their shapes. The two groups also differ in regard to their location in the superior olivary complex.

D-ASP-preferring OC neurons

The vast majority of D-ASP-labeled OC neurons are located within the LSO; no neuron labeled with WGA/HRP alone could be identified in this nucleus. Of the 55 individual D-ASP OC neurons examined in this study, 51 were located within the ipsilateral LSO, primarily in the middle and medial limbs; 2 were found in the contralateral LSO; and the remaining 2 were observed outside of the ipsilateral LSO, between its lateral limb and the lateral nucleus of the trapezoid body nearby. This distribution pattern reflects that described for the separate and larger number of D-ASP OC neurons studied light-microscopically by Ryan et al. (1987). All of the D-ASP-preferring neurons studied were similar enough to one another morphologically to be classed as a single neuronal population. D-ASP-labeled axons located within the LSO neuropil, presumably belonging to D-ASP OC neurons, were observed to be either lightly myelinated or unmyelinated.
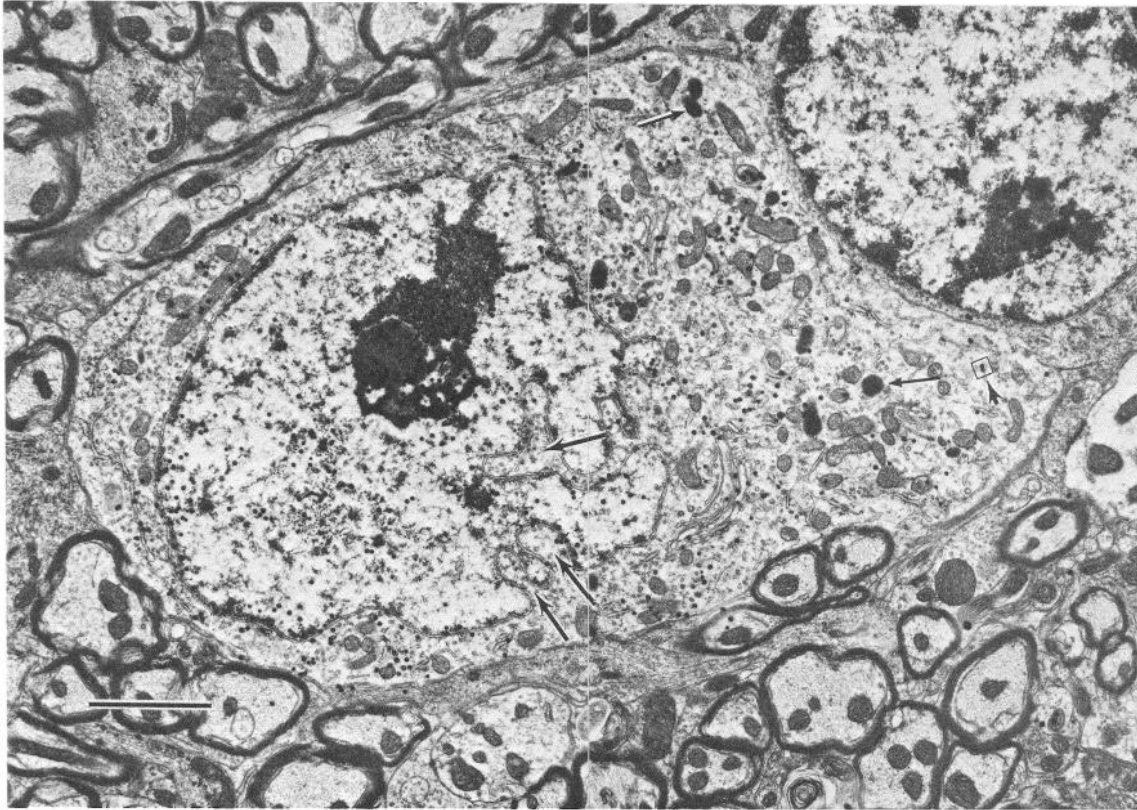
Figure 1. Montage of D-ASP-preferring OC neuron. This neuron possesses an eccentrically positioned nucleus with prominent nucleoplasmic infoldings (*large arrows*); its cytoplasm contains only small, disorderly arrays of rough endoplasmic reticulum. There are no presynaptic terminals contacting the perikaryon in this profile. Silver grains resulting from D-ASP decay can be seen over both the cytoplasm and nucleoplasm (2 of these grains are enclosed in the *box* indicated by the *arrowhead*). WGA/HRP granules (*small arrows*) can also be seen. Bar, 2 μm.

Systematic searching of all sections of LSO ipsilateral to the perfused cochleas identified 5 unlabeled perikarya that shared all morphological features common to the D-ASP-labeled profiles. Several possibilities could explain their presence: these neurons could be the source of the crossed projections to the contralateral cochlea; they might have been rendered incapable of retrograde uptake; or they could be entirely unrelated to the OC system.

The perikarya of the D-ASP-preferring OC neurons were typically oval or fusiform in shape. Nucleolus-containing profiles measured from 12 to 17 μm in length ($\bar{x} = 14.4$ μm; $s = 1.9$; $N = 16$) and from 7.8 to 12.5 μm in width ($\bar{x} = 9.3$; $s = 1.4$; $N = 16$). Perikaryal profiles of this class were often observed apposed to a single oligodendrocyte and/or its processes. The D-ASP OC neuron possesses little cytoplasm, within which can be found an eccentrically positioned nucleus with prominent nucleoplasmic infoldings (Fig. 1). These infoldings appear to be most abundant on the surface of the nucleus closest to a dendritic trunk. Silver grains resulting from D-ASP decay were found over both the cytoplasm and nucleoplasm. The cytoplasm of D-ASP OC neurons contains mostly small, disorderly arrays of rough endoplasmic reticulum, each array containing 1–5 cisternae, with their associated ribosomes set into polyribosomal rosettes. Occasionally a profile contained one larger, more elaborate Nissl body with stacks exceeding 5 cisternae.

The synaptic input to D-ASP-preferring OC neurons is generally sparse. Only a small percentage, if any, of the perikaryal surface of these neurons receives axosomatic input. Thirteen percent or less of the profiles of any given D-ASP-preferring neuron ($\bar{x} = 6.1\%$; $s = 4.0$; $N = 53$) is apposed to presynaptic terminals (Fig. 2A). Labeled dendritic cross sections with no synaptic appositions were frequently encountered; those bearing synapses most often possessed only one presynaptic terminal. According to observations on longitudinal profiles of labeled dendrites, presynaptic terminals were typically spaced more than 10 μm apart. The scarcity of axodendritic synapses was observed on labeled dendrites with diameters as small as 1 μm. By contrast, most of the surrounding, unlabeled dendritic profiles in the LSO were covered almost entirely by boutons. No distinction could be made between the somata and dendrites in the types and proportions of presynaptic terminals contacting the D-ASP-labeled cells.

Figure 2B (top) summarizes the classification and distribution of 75 synaptic terminals studied from D-ASP-preferring OC neurons. The vast majority of both axosomatic and axodendritic synapses possessed asymmetrical paramembranous thickenings, separated by a synaptic cleft measuring 25–30 nm in width. The presynaptic terminals contained small, round and/or oval vesicles, ranging in size from 30 to 40 nm, which were usually clustered near the active zones (Fig. 3, A–C); 41 of 68 of these terminals with mildly pleomorphic vesicles contained at least one dense core vesicle 70–100 nm in diameter (Fig. 3C). The 2 preterminal axons observed forming terminals of this type were unmyelinated (Fig. 3B). A second type of synapse, containing larger pleomorphic vesicles with major axes exceeding 40 nm (Fig. 4), was encountered rarely on either the somata or dendrites of D-ASP OC neurons. The paramembranous thickenings associated with these synapses appeared more punc-
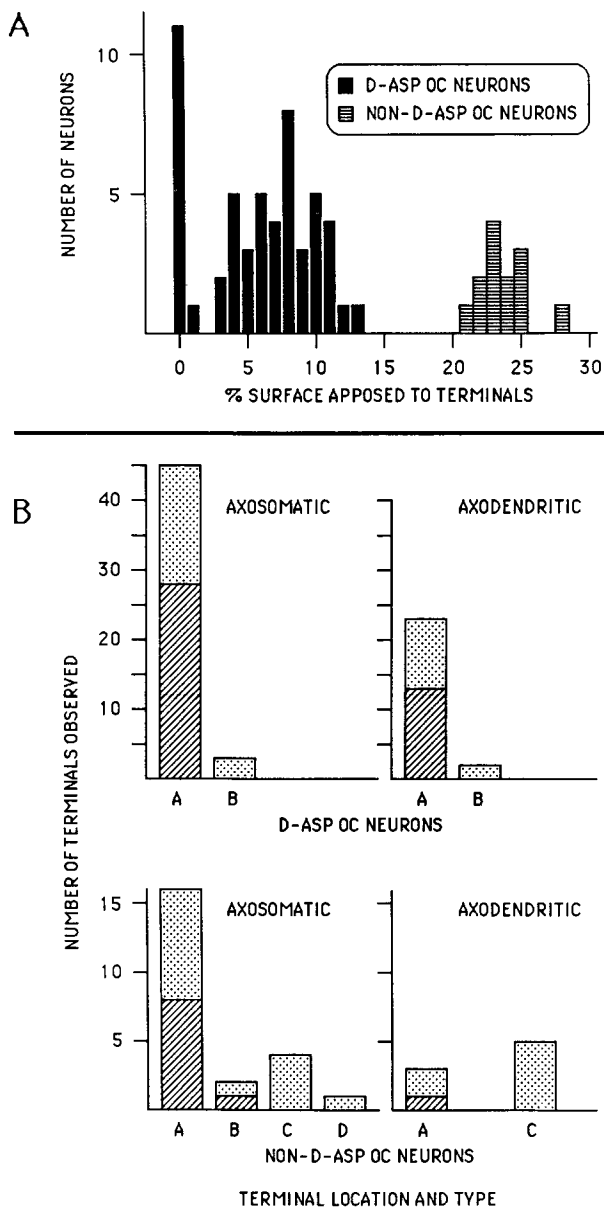
Figure 2. Percentages and distribution of synapses. *A,* Graph illustrating the percentage of perikaryal surface of OC neurons in apposition with synaptic terminals, from samples of 53 D-ASP-preferring and 13 non-D-ASP-preferring OC neurons. *B,* Distribution of synapses on D-ASP-preferring and non-D-ASP-preferring OC neurons. Type of presynaptic terminal is indicated as follows: *A,* terminals with 30–40 nm, mildly pleomorphic vesicles; *B,* terminals with ≥40 nm pleomorphic vesicles; *C,* terminals with 40–50 nm round vesicles; *D,* terminals containing ~30 nm round vesicles. *Slanted lines,* presynaptic terminals containing at least one dense core vesicle.

tate and less asymmetrical than those of the first category, and the synaptic cleft measured 20 nm in width.

The synaptic profiles on the D-ASP-labeled neurons differed markedly from those on most unlabeled cell types in the LSO. Most of the surface of the majority of unlabeled LSO perikarya was apposed to synaptic terminals that contained distinctly pleomorphic vesicles and slightly asymmetrical synaptic specializations, with fewer containing larger, round (40–50 nm) vesicles and distinctly asymmetrical paramembranous thickenings. The unlabeled dendritic profiles were contacted, in roughly equal

proportions, by the synapses with larger vesicles and those with pleomorphic vesicles. Very rarely, the smaller vesicle synapse (30–40 nm) was observed in contact either with the perikarya or with dendrites of unlabeled profiles.

Non-D-ASP-preferring OC neurons

Non-D-ASP-preferring neurons, labeled with WGA/HRP only, were found bilaterally outside of the LSO. Because these neurons were infrequently encountered at the light-microscopic level, only 13 neurons from this class were studied electron-microscopically. Six were located in the SOC ipsilateral to the perfused cochlea and 7 were located in the contralateral SOC. More specifically, 3 of the ipsilateral non-D-ASP-labeled OC neurons were located in the ventral nucleus of the trapezoid body (VNTB) and 3 were found in the area between the medial superior olive (MSO) and the medial nucleus of the trapezoid body (MNTB). Also, 4 neurons of this type were found in the contralateral VNTB, and 3 were identified contralaterally in the region between the MSO and MNTB. In one case, a neuron labeled only with WGA/HRP was observed, light-microscopically, medial to the medial limb of the LSO ipsilateral to the perfused cochlea (Fig. 5); however, it could not be located in the subsequent sections prepared for electron microscopy. Non-D-ASP-preferring OC neurons appeared to possess either a bipolar or multipolar dendritic organization, regardless of their location in the SOC. No other obvious cytological differences were noted among the non-D-ASP OC neurons.

Non-D-ASP OC neurons are larger than their D-ASP-labeled counterparts. Their lengths exceed 20 μm and their widths range from 10 to 20 μm, depending on whether the soma is fusiform or polygonal in shape. Their cytoplasm contains numerous large blocks of well-organized rough endoplasmic reticulum with smaller, less organized Nissl substance interspersed throughout (Fig. 6). The nucleus is usually eccentrically placed in the fusiform somata and centered in the polygonal perikarya of non-D-ASP OC cells, and possesses only a moderate degree of nucleoplasmic infolding when compared to D-ASP OC neurons.

Twenty to 30% of the surface of each non-D-ASP neuron profile studied was apposed to presynaptic terminals ($\bar{x}$ = 24.0%; s = 1.9; N = 13). These values were consistently greater than those for D-ASP OC neurons and allowed these 2 groups of OC neurons to be divided into separate populations based upon their axosomatic synaptic profiles (Fig. 2A). The lower portion of Figure 2B summarizes the classification and distribution of 31 synaptic terminals on the non-D-ASP neurons studied. Four types of axosomatic synapses were observed. The majority of presynaptic terminals contained round and/or oval vesicles 30–40 nm in diameter and asymmetrical synaptic specializations, with synaptic clefts measuring 25–30 nm wide (Fig. 7A); one-half of these terminals contained dense core vesicles. This type appeared similar to the one forming the vast majority of synapses on D-ASP OC neurons. Less frequently observed were synapses containing large, round vesicles, 40–50 nm in diameter, and prominent asymmetrical synaptic specializations separated by a 30 nm synaptic cleft (Fig. 8A); the terminal in Figure 8A receives a myelinated axon. Rarely seen were axosomatic synapses containing predominantly flat vesicles 40–60 nm in length (Fig. 8B). In addition, a single presynaptic terminal was observed contacting both a labeled and an unlabeled neuron in the ventral nucleus of the trapezoid body contralateral to the perfused cochlea (Fig. 7B); this type contained lucent and uniformly small, round vesicles 30 nm in diameter.
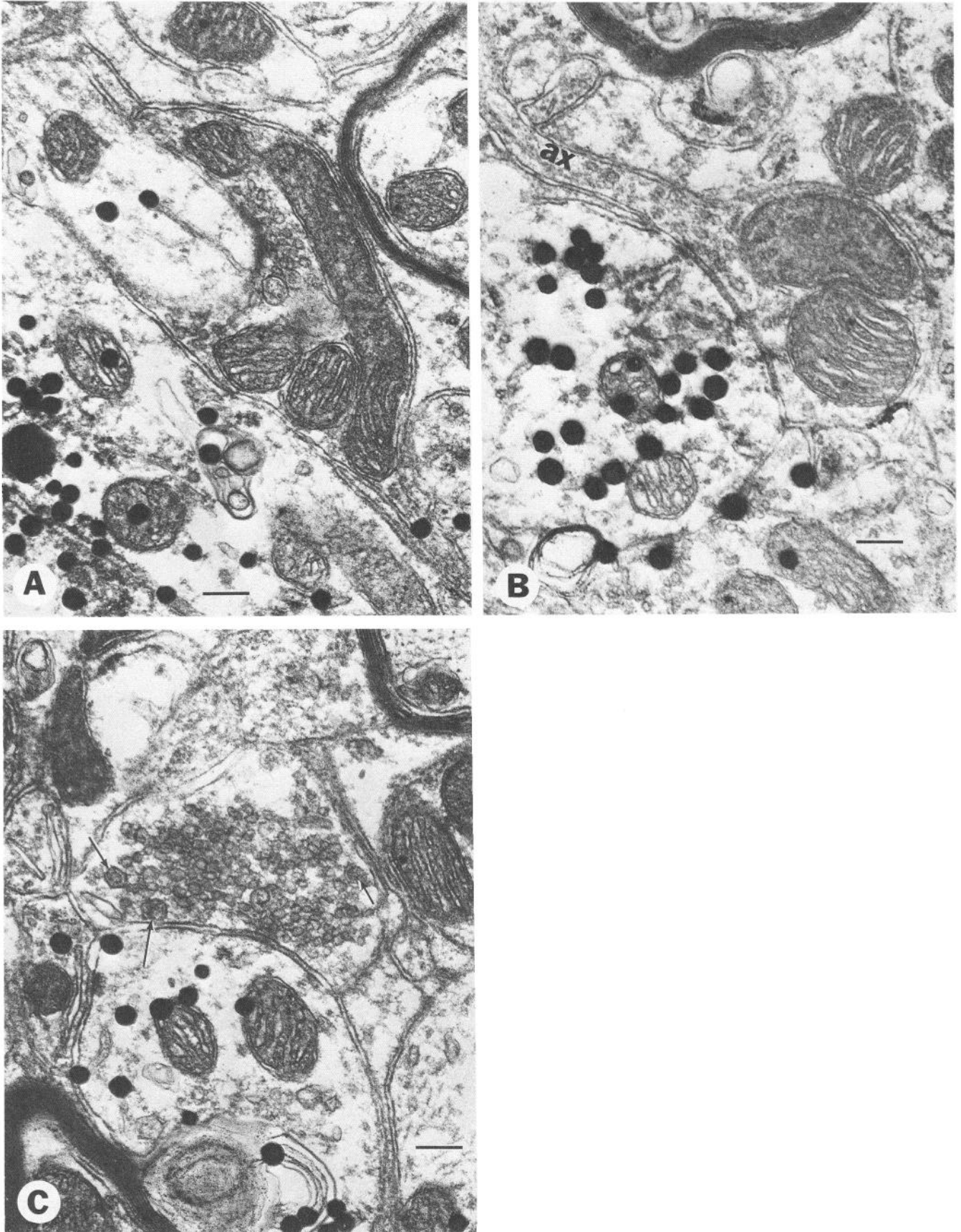
Figure 3. Synapses on D-ASP-preferring OC neurons that contain mildly pleomorphic 30–40 nm vesicles. An unmyelinated axon (*ax*) forming a presynaptic terminal can be seen in *B. Arrows* in *C* indicate dense core vesicles. Bars, 200 nm.
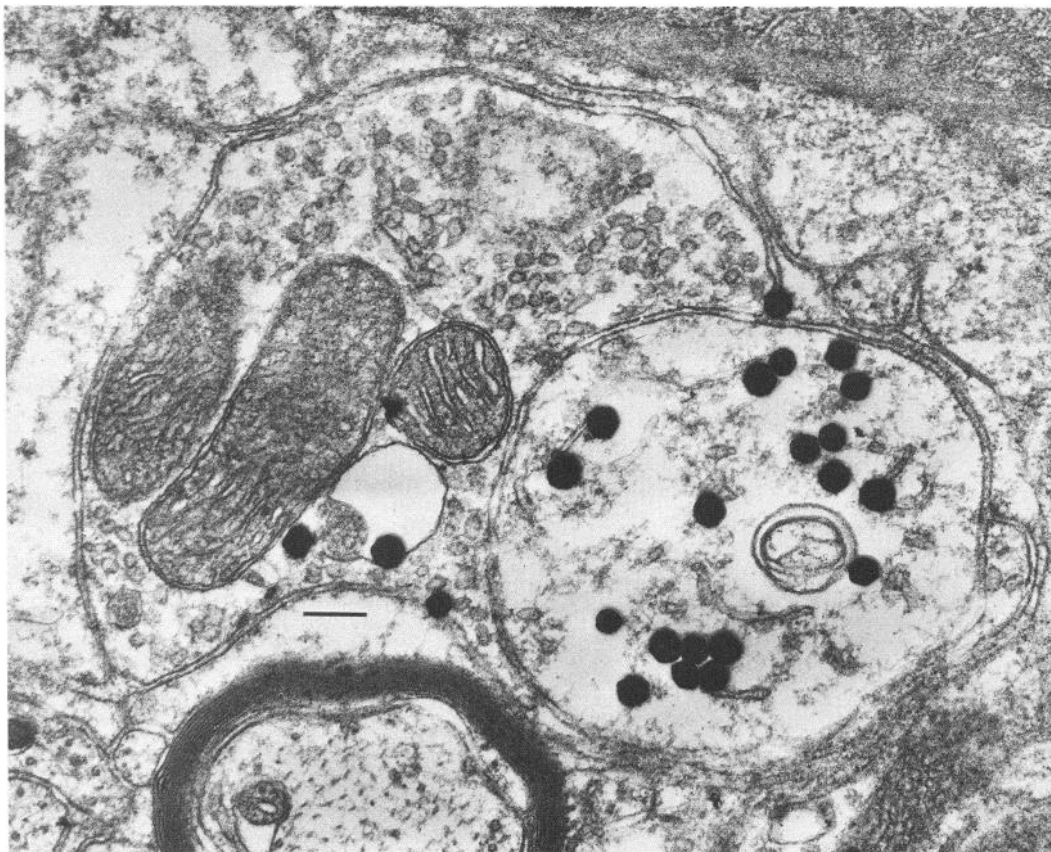
Figure 4. Axodendritic synapse on D-ASP-preferring OC neuron that contains pleomorphic vesicles larger than those found in Figure 3. Bar, 200 nm.

Most of the dendrites of non-D-ASP OC neurons were sparsely labeled with WGA/HRP granules. As a result, in most cases, only proximal dendrites observed attached to the labeled somata could be identified as belonging to the non-D-ASP OC neurons and analyzed for synaptic contacts. Eight axodendritic synapses were observed on the non-D-ASP OC neurons. Five of the presynaptic terminals contained 40–50 nm round vesicles, and the remaining 3 contained the 30–40 nm round/oval vesicles. Both types of axodendritic synapses appeared to correspond to those similarly described on the perikarya. Although the sample was very small, there appeared to be a difference in the relative proportions of the synaptic classes contacting the perikarya and dendrites of non-D-ASP OC neurons. This was not the case for D-ASP OC neurons, where differences in the proportions of synaptic types between the dendrites and cell body were negligible.

Discussion

This study provides the first detailed description of the ultrastructural characteristics, including the distribution and morphology of the synaptic terminals incident on their somas and dendrites, of 2 classes of gerbil OC neurons that are distinguished from each other by their ability to accumulate and retrogradely transport D-ASP from the cochlea. These 2 classes can also be distinguished from one another morphologically as well as by their distribution within the superior olivary complex, and correspond well to the previously described lateral and medial systems of OC neurons. The observation of multiple

classes of synapses contacting both types of OC neurons suggests that each type may receive input from more than one source.

The OC neurons capable of uptake and retrograde transport of D-ASP are located within, or very near, the LSO. They are small and fusiform, contain a small amount of cytoplasm with scant, poorly organized Nissl substance, and possess a nucleus with deep infoldings. The D-ASP OC neurons receive very few synapses, the vast majority of which contain small, mildly pleomorphic synaptic vesicles and asymmetrical synaptic specializations; most of these synapses also contain a small number of dense core vesicles. Rarely observed on these neurons were synapses with larger pleomorphic vesicles and only slightly asymmetrical synaptic specializations. Most D-ASP OC neurons project to the ipsilateral cochlea.

OC neurons unable to preferentially accumulate D-ASP have a more bilateral distribution and are located primarily in the VNTB, and in the area between the MSO and MNTB. They are larger than the D-ASP-preferring OC neurons and there is a greater variation in their shape, which ranges from fusiform and bipolar to polygonal and multipolar in transverse sections. However, despite this variation in shape, all of the non-D-ASP neurons studied possess similar cytoplasmic and nuclear features, as well as similar types, proportions, and distributions of synapses. Their cytoplasm contains large blocks of Nissl substance and a nucleus with moderate infoldings. A greater percentage of their surfaces is apposed to presynaptic terminals, as compared to D-ASP OC neurons. Four types of synapses can be identified on non-D-ASP OC neurons, 2 of which predominate.
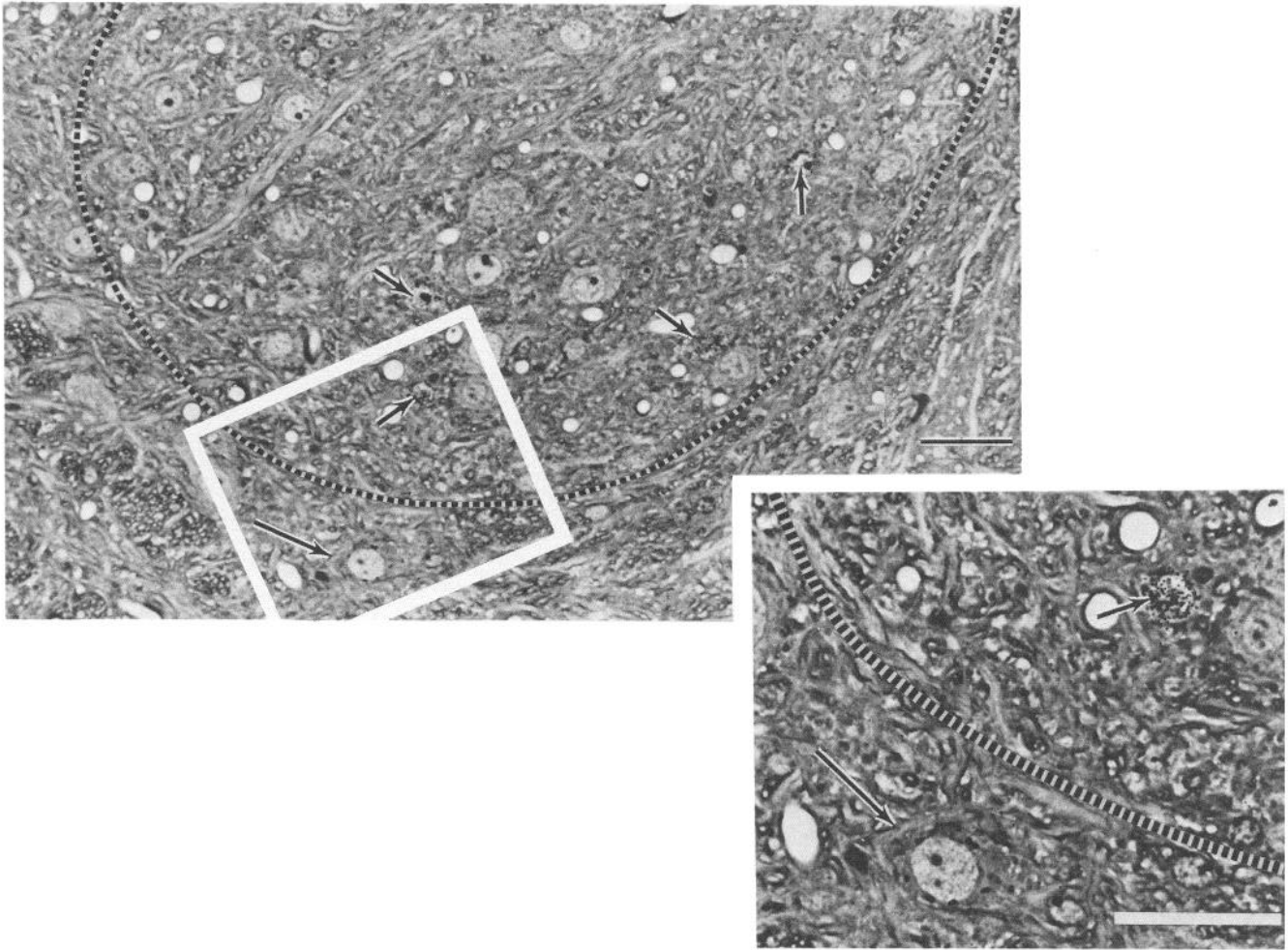
Figure 5. D-ASP-preferring OC neurons (*short arrows*) can be seen within the medial limb of the LSO (*enclosed in broken line*), while a single non-D-ASP-preferring OC neuron (*long arrow*) is located immediately outside of the LSO. The *top* is directed laterally, the *right side* is directed dorsally. *Inset* is an enlargement of the area enclosed in the box. Bars, 30 μm.

Most abundant on the perikarya are synapses with small, mildly pleomorphic vesicles with asymmetrical synaptic specializations (very similar in appearance to the ones commonly seen on the D-ASP OC neurons). Roughly one-half of the profiles of these synapses also contain dense core vesicles. The synapses most commonly observed on the dendrites are those containing large, round vesicles and asymmetrical paramembranous thickenings. The remaining 2 synaptic types are much less frequently encountered; one contains small, round vesicles and the other predominantly flat vesicles.

Association of D-ASP-preferring OC neurons with the LOC system

The confinement of the vast majority of D-ASP OC neurons to the LSO, with the remaining few found immediately outside of its lateral limb, agrees with the light-microscopic observations on the distribution of D-ASP OC neurons in the gerbil by Ryan et al. (1987). The morphology of D-ASP-preferring OC neurons at the electron-microscopic level, and their distribution within the LSO, corresponds precisely to that described for the small neurons by Helfert and Schwartz (1986). All of the ultrastructural features of the gerbil D-ASP OC neurons are similar to those described for the LOC neurons residing within or near

the LSO of the rat (White, 1983, 1986), guinea pig (Strutz and Bielenberg, 1983), and cat (Spangler et al., 1985, 1986). They are also similar to the small neurons described in the cat LSO neuropil (Cant, 1984; Helfert and Schwartz, 1986); however, the relationship between small neurons and LOC neurons in this species is still unknown. Class 5 neurons of the LSO, similar in appearance to MOC neurons, were labeled by neither D-ASP nor WGA/HRP; thus, although they share a distribution within the gerbil LSO similar to that of the smaller D-ASP-labeled OC neurons, the class 5 neurons apparently do not provide direct efferent innervation to the inner ear. Whether their similarities in distribution imply a functional relationship between class 5 neurons and the D-ASP OC neurons, or are merely coincidental, remains to be determined.

Little doubt should remain that the population of D-ASP-preferring OC neurons is the principal component of the gerbil LOC system. The morphology and distribution of D-ASP OC neurons fit the description for LOC neurons as stated above; their axons within the brain stem are unmyelinated (Ryan et al., 1987) or, at the most, lightly myelinated, and the association of these neurons with the D-ASP-labeled terminals observed beneath the gerbil inner hair cells (Schwartz and Ryan, 1986), the primary target of LOC neurons, is clear (Ryan et al., 1987).
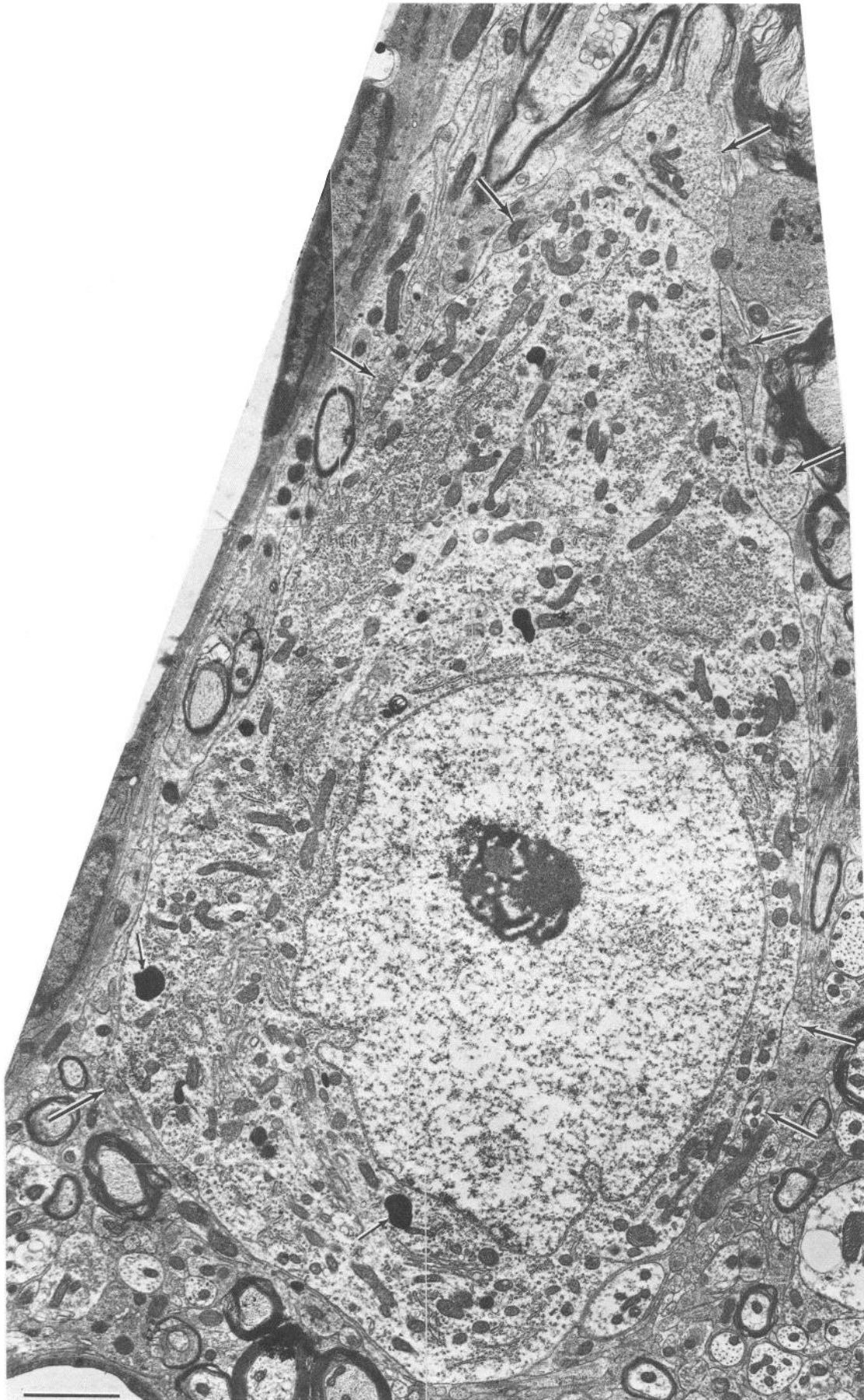
Figure 6. Montage of non-D-ASP-preferring OC neuron. The cytoplasm of this neuron contains numerous blocks of well-organized rough endoplasmic reticulum with smaller, less organized Nissl substance interspersed throughout. Axosomatic contacts can be observed (*large arrows*). Two WGA/HRP granules are indicated (*small arrows*). Bar, 2 μm.
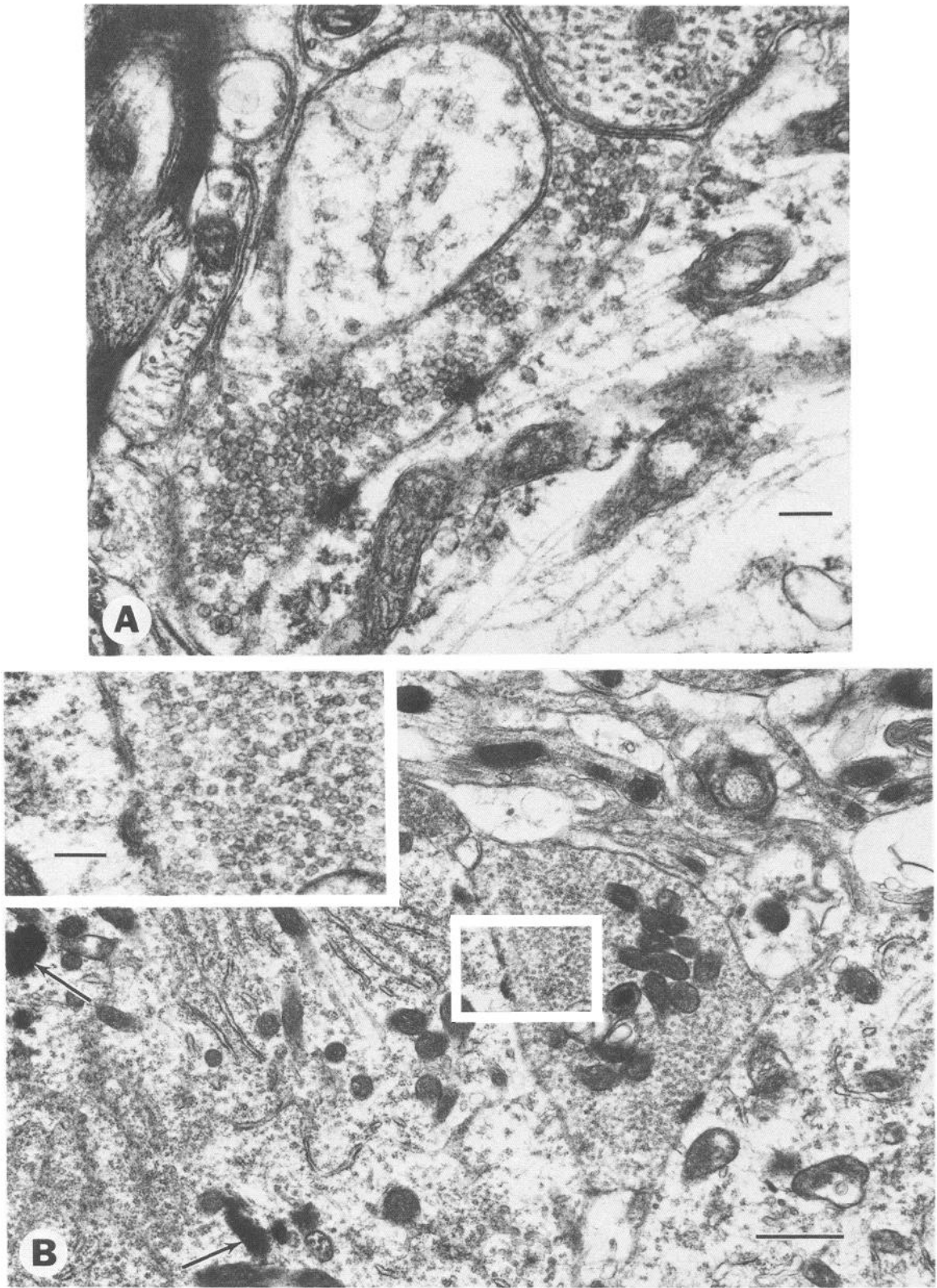
Figure 7. Synapses occurring on non-D-ASP-preferring OC neurons. *A,* Synapse with 30–40 nm pleomorphic vesicles and a few 70–100 nm dense core vesicles. *B,* Synapse with small (30 nm), round vesicles contacting 2 perikarya. WGA/HRP granules can be seen in the soma to the left of the synapse (*arrows*). Bar, 1 μm. *Inset,* an enlargement of the area enclosed in the box. Bar, 200 nm.
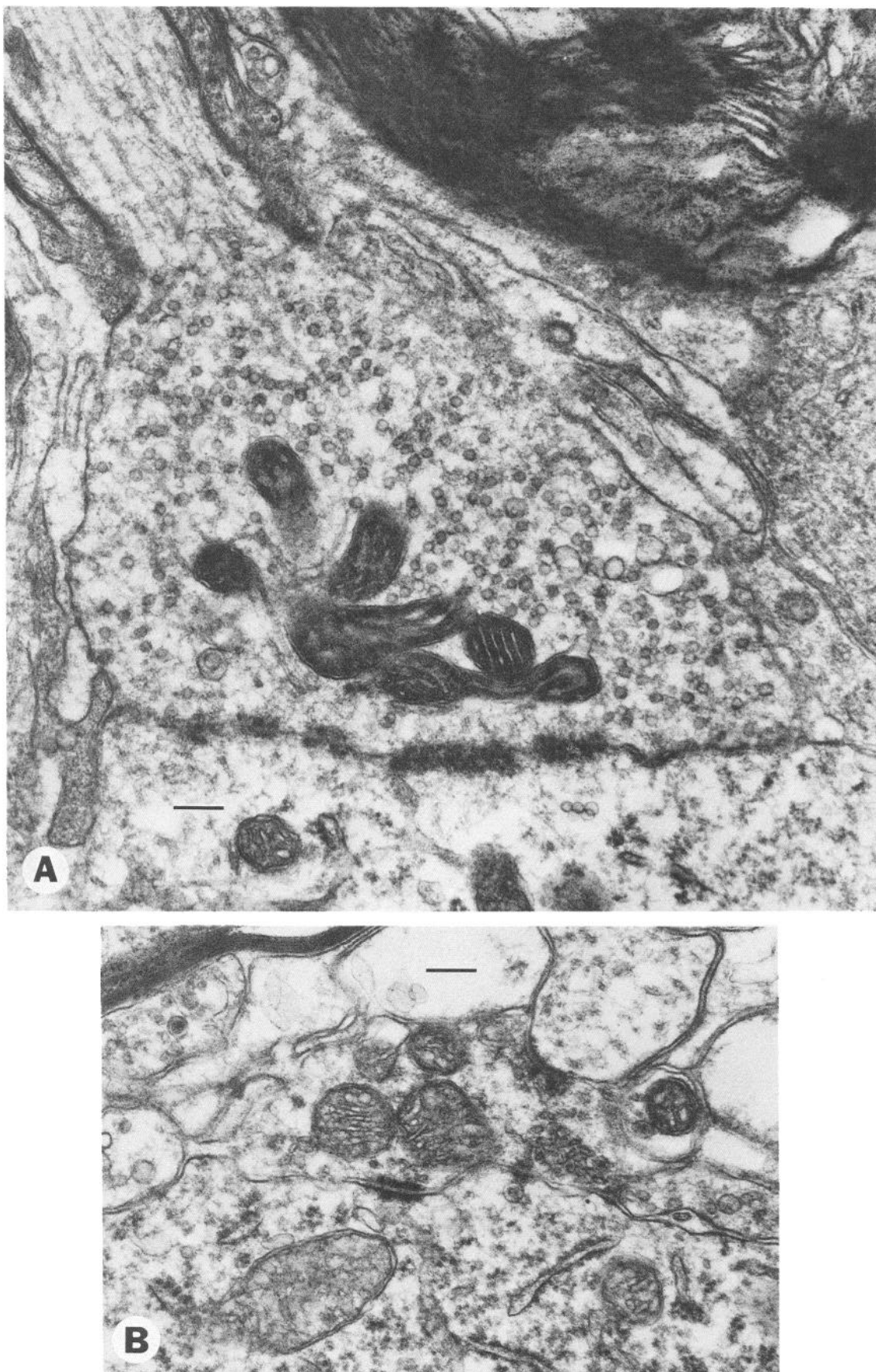
Figure 8. Synapses on non-D-ASP-preferring OC neurons. *A,* Large (40–50 nm), round vesicle synapse. *B,* Synapse containing elongated (flat) vesicles and a dense core vesicle. Bars, 200 nm.

Association of non-D-ASP-preferring neurons with the MOC system

The non-D-ASP-preferring OC neurons are located, bilaterally, in the VNTB and in the area between the MSO and MNTB, which corresponds to the location of MOC neurons in the gerbil (Ryan et al., 1986). These neurons differ little, ultrastructurally, from their counterparts as described in the rat (White, 1984, 1986) and cat (Spangler et al., 1985, 1986). In particular, the shape and cytoplasmic features of the MOC neurons of the species studied are very similar. A minor difference (and probably of equally minor significance) may be between the degree of nuclear infolding of the MOC neurons of the rat (White, 1984) and the non-D-ASP-preferring MOC neurons of the gerbil observed in this study. The rat MOC neurons apparently exhibit a greater magnitude of nucleoplasmic indentation (White, 1984) than do the gerbil non-D-ASP MOC neurons.

Of greater significance are the potential differences between the types of synaptic input contacting the cat and rat MOC neurons and the gerbil non-D-ASP MOC neurons. Spangler et al. (1986) noted that most of the presynaptic terminals contacting the cat MOC neurons contained mostly pleomorphic vesicles with scattered dense core vesicles, and that the remaining few terminals contained flat vesicles; no large, round vesicle terminals were observed. In contrast, White (1984, 1986) found that the majority of axon terminals contacting rat MOC neurons contained a population of either large or small round vesicles, and that a small percentage of terminals contained mainly flat or elongated vesicles. The present study identified 4 types of terminals contacting gerbil non-D-ASP OC neurons, as described above. The absence of large, round vesicle synapses on cat MOC neurons suggests that the synaptic input to the cat MOC neurons differs in this regard from that of the rat and gerbil, whose MOC neurons do receive synapses of this type. The ability to interpret the remaining interspecific differences among the synaptic profiles of the MOC neurons is limited; the studies on the cat and rat are at present available only in abstract form, with no illustrations, vesicle dimensions, or relative proportions of synaptic types available for comparison with the gerbil data in this study.

Potential sources and neurotransmitter roles for the synaptic types contacting OC neurons

Identification of the sources of the morphologically distinct types of synapses contacting OC neurons and the putative neurotransmitters associated with them is beyond the scope of this study. However, neurotransmitter candidates have been associated with synapses elsewhere in the brain stem and can be compared to auditory synaptic types with similar features.

The mildly pleomorphic vesicle synapses commonly observed on both classes of OC neurons appear similar, morphologically, to the GABA-immunoreactive pleomorphic "oval" synapses described in the guinea pig ventral cochlear nucleus (VCN) (Altschuler et al., 1986b) and superior olivary complex (SOC) (Helfert et al., 1988). This similarity suggests that the mildly pleomorphic vesicle OC synapses may be GABAergic. In the auditory brain stem, GABA-immunoreactive perikarya can be found in the VCN (Wenthold et al., 1986; Schwartz et al., 1987), SOC (Peyret et al., 1986; Helfert et al., 1987), and inferior colliculus (Roberts et al., 1985a, b; Caspary and Lawhorn, 1987). Since neurons in these locations are known to project to the SOC (Stotler, 1953; Harrison and Warr, 1962; van Noort, 1969; Warr,

1982), these sites are potential sources of GABA synapses on OC neurons, if GABAergic input does indeed exist.

The large pleomorphic vesicle synapses on OC neurons are similar in appearance to the flat vesicle synapses described in the cat LSO (Cant, 1984; Helfert and Schwartz, 1986), which are thought to be glycinergic (Schwartz, 1983a; Cant, 1984; Helfert et al., 1987). They are also similar to the glycine (GLY)-immunoreactive flat vesicle synapses identified in the guinea pig VCN (Altschuler et al., 1986c). A source of the glycinergic input to the LSO and, perhaps, to the OC neurons is hypothesized to originate from the principal cells of the medial nucleus of the trapezoid body (Moore and Caspary, 1983). An additional source of glycinergic input could be from the VCN, where 2 populations of GLY-immunopositive neurons reside (Wenthold et al., 1987).

The large vesicle synapses on the medial OC neurons resemble those found on the dendrites of LSO neurons in the cat (Cant, 1984; Helfert and Schwartz, 1986) and gerbil (Helfert and Schwartz, 1987). Large vesicle synapses also form the endbulb synapses on the spherical cells of the anteroventral cochlear nucleus (Gulley et al., 1978; Cant and Morest, 1979). These synapses exhibit immunoreactivity in the presence of antibodies to enzymes believed to be involved in the production of the excitatory amino acids, aspartate and glutamate (Altschuler et al., 1981, 1984b), although they do not accumulate tritiated aspartate and glutamate in brain slice preparations (Schwartz, 1983b). The spherical and globular neurons of the VCN are thought to provide this input to the SOC (Warr, 1966, 1972, 1982; Cant, 1984), which could include neurons of the MOC system.

Small, round vesicle synapses have been identified in the LSO of the cat (Cant, 1984), as well as on the MOC neurons. Studies by McDonald and Rasmussen (1971) have identified acetylcholinesterase-stained small vesicle synapses in the AVCN, suggesting that these synapses may be cholinergic. Small, round vesicle synapses could come from neurons of the olivocochlear system itself, as there is evidence that the neurons of both systems are the only ones in the SOC that are cholinergic (Osen and Roth, 1969; Warr, 1975; Osen et al., 1984).

Do the gerbil LOC and MOC systems each contain only one neuronal class?

There is variation in the shape and dendritic organization among the cells within the population of gerbil non-D-ASP MOC neurons; some of these neurons appear fusiform and bipolar, while the remainder are polygonal and multipolar. Similar variation has been documented among the MOC neurons in the cat (Adams, 1983; Spangler et al., 1985). Yet, at the ultrastructural level, both cytologically and synaptologically, gerbil non-D-ASP OC neurons appear to belong to a single neuronal class. The functional consequences that might be brought about by the differences in shape or dendritic organization between gerbil MOC neurons are not obvious.

The D-ASP LOC neurons form a morphologically homogeneous population and constitute the vast majority, if not the entire population, of LOC cells. However, 2 findings suggest that these neurons do not compose the entire LOC population. First, a non-D-ASP OC neuron located immediately outside of the medial limb of the LSO, a site seemingly within the boundaries established for LOC neurons, was identified in this study. This neuron appeared larger than the LOC neurons, more similar in size to MOC neurons. Unfortunately, this cell was ob-

served only at the light-microscopic level, so its ultrastructural features could not be compared to those of MOC neurons. Second, a very small number of LOC neurons dorsal to the LSO were labeled after cochlear perfusions with ³H-nipecotic acid (NIP), a GABA analog (Ryan et al., 1986). This compound was also identified bilaterally in the MOC neurons. No D-ASP OC neurons were identified in these regions by this study or by Ryan et al. (1987). These findings suggest that a small population of non-D-ASP LOC neurons preferentially accumulates NIP from the cochlea. Neurons dorsal to the LSO were not seen in this study, probably because of our small sample size and their rarity, so comparisons between these neurons and MOC neurons in the gerbil could not be made. Electron-microscopic studies involving the uptake of NIP from the cochlea are currently under way and may identify this small population of neurons, so that it can be analyzed and placed in the proper context of what is now known about the gerbil OC system.

References

Adams, J. C. (1983) Cytology of periolivary cells and the organization of their projections in the cat. J. Comp. Neurol. 215: 275–289.

Adams, J. C. (1986) Cells of origin of cochlear efferents in human. Assoc. Res. Otolaryngol. Abstr. 9: 5.

Altschuler, R. A., G. R. Neises, G. G. Harmison, R. J. Wenthold, and J. Fex (1981) Immunocytochemical localization of aspartate aminotransferase immunoreactivity in cochlear nucleus of the guinea pig. Proc. Natl. Acad. Sci. USA 78: 6553–6557.

Altschuler, R. A., M. H. Parakkal, and J. Fex (1983) Localization of enkephalin-like immunoreactivity in acetylcholinesterase positive cells in the guinea pig lateral superior olivary complex that project to the cochlea. Neuroscience 9: 621–630.

Altschuler, R. A., J. Fex, M. H. Parakkal, and F. Eckenstein (1984a) Colocalization of enkephalin-like and choline acetyltransferase-like immunoreactivities in olivocochlear neurons of the guinea pig. J. Histochem. Cytochem. 32: 839–843.

Altschuler, R. A., R. J. Wenthold, A. M. Schwartz, W. G. Haser, N. P. Curthoys, M. Parakkel, and J. Fex (1984b) Immunocytochemical localization of glutaminase-like immunoreactivity in the auditory nerve. Brain Res. 291: 173–178.

Altschuler, R. A., N. Jones, K. A. Reeks, and J. Fex (1986a) Tyrosine hydroxylase immunoreactivity marks a catecholaminergic system in the guinea pig organ of Corti. Assoc. Res. Otolaryngol. Abstr. 9: 91.

Altschuler, R. A., D. W. Hoffman, and R. J. Wenthold (1986b) Neurotransmitters of the cochlea and cochlear nucleus: Immunocytochemical evidence. Am. J. Otolaryngol. 7: 100–106.

Altschuler, R. A., H. Betz, M. H. Parakkal, K. A. Reeks, and R. J. Wenthold (1986c) Identification of glycinergic synapses in the cochlear nucleus through immunocytochemical localization of the glycine receptor. Brain Res. 369: 316–320.

Arneson, A. R., and K. K. Osen (1984) Fibre population of the vestibulocochlear anastomosis in the cat. Acta Otolaryngol. 98: 255–269.

Bobbin, R. P., and T. Konishi (1971) Acetylcholine mimics crossed olivocochlear bundle stimulation. Nature 231: 222–223.

Cant, N. B. (1984) The fine structure of the lateral superior olivary nucleus of the cat. J. Comp. Neurol. 227: 63–77.

Cant, N. B., and D. K. Morest (1979) The bushy cells in the anteroventral cochlear nucleus of the cat: A study with the electron microscope. Neuroscience 4: 1925–1945.

Caspary, D. M., and B. A. Lawhorn (1987) Loss of GABA-immunoreactive neurons in the inferior colliculus of the aged rat. Soc. Neurosci. Abstr. 13: 545.

Eybalin, M., and R. Pujol (1984) Immunofluorescence with met-enkephalin and leu-enkephalin antibodies in the guinea pig cochlea. Hearing Res. 12: 135–140.

Fex, J., and R. A. Altschuler (1981) Enkephalin-like immunoreactivity of olivocochlear nerve fibers in the cochlea of guinea pig and cat. Proc. Natl. Acad. Sci. USA 78: 1255–1259.

Fex, J., R. A. Altschuler, R. J. Wenthold, and M. H. Parakkal (1982a) Aspartate aminotransferase immunoreactivity in cochlea of guinea pig. Hearing Res. 7: 149–160.

Fex, J., R. A. Altschuler, M. H. Parakkal, and F. Eckenstein (1982b)

Immunocytochemical localization of choline acetyltransferase-like immunoreactivity in olivocochlear fibers in the guinea pig cochlea. Soc. Neurosci. Abstr. 8: 41.

Guinan, J. J., W. B. Warr, and B. E. Norris (1983) Differential olivocochlear projections from the lateral versus medial zones of the superior olivary complex. J. Comp. Neurol. 221: 358–370.

Guinan, J. J., W. B. Warr, and B. E. Norris (1984) Topographic organization of the olivocochlear projections from the lateral and medial zones of the superior olivary complex. J. Comp. Neurol. 226: 21–27.

Gulley, R. L., D. M. A. Landis, and T. S. Reese (1978) Internal organization of the endbulbs of Held in the anteroventral cochlear nucleus. J. Comp. Neurol. 180: 707–742.

Harrison, J. M., and W. B. Warr (1962) The cochlear nucleus and ascending pathways of the medulla. J. Comp. Neurol. 119: 341–380.

Helfert, R. H., and I. R. Schwartz (1986) Morphological evidence for the existence of multiple neuronal classes in the cat lateral superior olivary nucleus. J. Comp. Neurol. 244: 533–549.

Helfert, R. H., and I. R. Schwartz (1987) Morphological features of five neuronal classes in the gerbil lateral superior olive. Am. J. Anat. 179: 55–69.

Helfert, R. H., I. R. Schwartz, and A. F. Ryan (1986) Ultrastructural characterization of olivocochlear efferent neurons in the gerbil lateral superior olive labeled retrogradely by uptake of ³H-D-aspartic acid and/or horseradish peroxidase from the cochlea. Soc. Neurosci. Abstr. 12: 1270.

Helfert, R. H., R. A. Altschuler, and R. J. Wenthold (1987) GABA and glycine immunoreactivity in the guinea pig superior olivary complex. Soc. Neurosci. Abstr. 13: 544.

Helfert, R. H., J. M. Bonneau, R. J. Wenthold, and R. A. Altschuler (1988) Ultrastructural characterization of GABA and glycine immunoreactive synapses in the guinea pig superior olivary complex. Soc. Neurosci. Abstr. (in press).

Itoh, K., A. Konishi, S. Nomura, N. Mizuno, Y. Nakamura, and T. Sugimoto (1979) Application of coupled oxidation reaction to electron microscopic demonstration of horseradish peroxidase: Cobalt–glucose oxidase method. Brain Res. 175: 341–346.

Jasser, A., and P. S. Guth (1973) The synthesis of acetylcholine by the olivocochlear bundle. J. Neurochem. 20: 45–54.

Karnovsky, M. J. (1967) The ultrastructural basis of capillary permeability studied with peroxidase as a tracer. J. Cell Biol. 35: 213–236.

Liberman, M. C. (1980) Efferent synapses in the inner hair-cell area of the cat cochlea: An electron microscopic study of serial sections. Hearing Res. 3: 189–204.

McDonald, D. M., and G. L. Rasmussen (1971) Ultrastructural characteristics of synaptic endings in the cochlear nucleus having acetylcholinesterase activity. Brain Res. 28: 1–18.

Moore, M. J., and D. M. Caspary (1983) Strychnine blocks binaural inhibition in lateral superior olivary neurons. J. Neurosci. 3: 237–242.

Morest, K., M. Ostapoff, J. Feng, and S. Kuwada (1986) Intracellular recordings of acoustic responses of identified cell types in the cochlear nucleus of the Mongolian gerbil and signs of a naturally occurring disease of the auditory system. International Union of Physiological Science Satellite Symposium on Hearing, University of California, San Francisco, CA, USA, p. 80 (abstr.).

Nuttall, A. L., D. M. Marques, and M. Lawrence (1977) Effects of perilymphatic perfusion with neomycin on the cochlea microphonic potential in the guinea pig. Acta Otolaryngol. 83: 393–400.

Osen, K. K., and K. Roth (1969) Histochemical localization of cholinesterases in the cochlear nuclei of the cat, with notes on the origin of acetylcholinesterase-positive afferents and the superior olive. Brain Res. 16: 165–185.

Osen, K. K., E. Mugnaini, A.-L. Dahl, and A. H. Christiansen (1984) Histochemical localization of acetylcholinesterase in the cochlear and superior olivary nuclei. A reappraisal with emphasis on the cochlear granule cell system. Arch. Ital. Biol. 122: 169–212.

Ostapoff, E. M., D. K. Morest, J. Feng, and S. Kuwada (1987) A degenerative disease of the auditory system of the gerbil, Meriones sp. Assoc. Res. Otolaryngol. Abstr. 10: 209.

Peyret, D., M. Geffard, and J.-M. Aran (1986) GABA immunoreactivity in the primary nuclei of the auditory central nervous system. Hearing Res. 23: 115–121.

Rasmussen, G. L. (1946) The olivary peduncle and other fiber connections of the superior olivary complex. J. Comp. Neurol. 84: 141–219.

Rasmussen, G. L. (1960) Efferent fibers of cochlear nerve and cochlear nucleus. In *Neural Mechanisms of the Auditory and Vestibular Systems*, G. L. Rasmussen and W. F. Windle, eds., pp. 105–115, Thomas, Springfield, IL.

Roberts, R. C., C. E. Ribak, L. M. Kitzes, and W. H. Oertel (1985a) Regional distribution of GABAergic neurons and axon terminals in the brainstem auditory nuclei of the gerbil. Anat Rec. *211:* 161A.

Roberts, R. C., C. E. Ribak, and W. H. Oertel (1985b) Increased numbers of GABAergic neurons occur in the inferior colliculus of an audiogenic model of genetic epilepsy. Brain Res. *361:* 324–338.

Ryan, A. F., N. K. Woolf, and F. R. Sharp (1982) Functional ontogeny in the central auditory pathway of the Mongolian gerbil: A deoxyglucose study. Exp. Brain Res. *47:* 428–436.

Ryan, A. F., I. R. Schwartz, and R. H. Helfert (1986) Nipecotic acid: Preferential retrograde labeling of a subpopulation of olivocochlear neurons following accumulation by GABA uptake systems in the cochlea. Soc. Neurosci. Abstr. *12:* 780.

Ryan, A. F., I. R. Schwartz, R. H. Helfert, E. Keithley, and Z.-X. Wang (1987) Selective retrograde labeling of lateral olivocochlear neurons in brainstem based on preferential uptake of ^{3}H-D-aspartic acid in the cochlea. J. Comp. Neurol. *255:* 606–616.

Schwartz, I. R. (1983a) Autoradiographic evidence that glycine labeling of synaptic terminals in the superior olivary complex has transmitter-like properties. In *Mechanisms of Hearing*, W. R. Webster and L. M. Aitkins, eds., p. 147, Monash U. P., Sydney, Australia.

Schwartz, I. R. (1983b) Differential uptake of H3-amino acids in the cat cochlear nucleus. Am. J. Otol. *4:* 300–304.

Schwartz, I. R., and P. D. Bok (1979) Electron microscopic localization of $^{125}\alpha$-bungarotoxin sites in the outer plexiform layer of the goldfish retina. J. Neurocytol. *8:* 53–66.

Schwartz, I. R., and A. F. Ryan (1986) Amino acid labeling patterns in the efferent innervation of the cochlea: An electron microscopic autoradiographic study. J. Comp. Neurol. *246:* 500–512.

Schwartz, I. R., S.-M. Yu, and G. Dicarlantonio (1987) A comparison of GABA and glycine immunoreactivity in the gerbil dorsal cochlear nucleus. Soc. Neurosci. Abstr. *13:* 544.

Schweitzer, L. F., S. M. Lu, D. Dawbarn, and N. B. Cant (1985) Calcitonin gene-related immunoreactivity in the superior olivary complex of cat and rat: A specific label for the lateral olivocochlear system. Soc. Neurosci. Abstr. *11:* 1051.

Spangler, K. M., J. S. White, and W. B. Warr (1985) The light and electron microscopic features of olivocochlear neurons in the cat. Anat. Rec. *211:* 182A.

Spangler, K. M., J. S. White, and W. B. Warr (1986) Electron microscopic features of axon terminals on olivocochlear neurons in the cat. Assoc. Res. Otolaryngol. Abstr. *9:* 37–38.

Stotler, W. A. (1953) An experimental study of the cells and connections of the superior olivary complex of the cat. J. Comp. Neurol. *98:* 401–432.

Strominger, N. L., S. M. Silver, T. C. Truscott, and J. C. Goldstein (1981) The cells of origin of the olivocochlear bundle in New and Old World monkeys. Anat. Rec. *199:* 246.

Strutz, J., and K. Bielenberg (1983) Efferent acoustic neurons within the lateral superior nucleus of the guinea pig. Brain Res. *299:* 174–177.

Thompson, G. C., A. M. Cortez, and M. Igarashi (1984) AChE neurons in the superior olivary complex of guinea pigs and squirrel monkeys. Assoc. Res. Otolaryngol. Abstr. *7:* 26–27.

van Noort, J. (1969) *The Structure and Connections of the Inferior Colliculus. An Investigation of the Lower Auditory Brainstem,* Van Gorcum, The Netherlands.

Warr, W. B. (1966) Fiber degeneration following lesions in the anterior-ventral cochlear nucleus of the cat. Exp. Neurol. *14:* 453–474.

Warr, W. B. (1972) Fiber degeneration following lesions in the multipolar and globular cell areas in the ventral cochlear nucleus of the cat. Brain Res. *40:* 247–270.

Warr, W. B. (1975) Olivocochlear and vestibular efferent neurons of the feline brain stem: Their location, morphology and number determined by retrograde axonal transport and acetylcholinesterase histochemistry. J. Comp. Neurol. *161:* 159–182.

Warr, W. B. (1978) The olivocochlear bundle: Its origins and terminations in the cat. In *Evoked Electrical Activity in the Auditory Nervous System,* R. F. Naunton and C. Fernandez, eds., pp. 43–65, Academic, New York.

Warr, W. B. (1982) Parallel ascending pathways from the cochlear nucleus: Neuroanatomical evidence of functional specialization. Contrib. Sensory Physiol. *7:* 1–38.

Warr, W. B., and J. J. Guinan (1979) Efferent innervation of the organ of Corti: Two separate systems. Brain Res. *173:* 152–155.

Warr, W. B., J. S. White, and M. J. Nyffeler (1982) Olivocochlear neurons: Quantitative comparison of the lateral and medial systems in adult and newborn cats. Soc. Neurosci. Abstr. *8:* 346.

Warr, W. B., J. J. Guinan, and J. S. White (1986) Organization of the efferent fibers: The lateral and medial olivocochlear systems. In *Neurobiology of Hearing: The Cochlea,* R. A. Altschuler, R. P. Bobbin, and D. W. Hoffman, eds., pp. 333–348, Raven, New York.

Wenthold, R. J., J. M. Zempel, M. H. Parakkal, K. A. Reeks, and R. A. Altschuler (1986) Immunocytochemical localization of GABA in the cochlear nucleus of the guinea pig. Brain Res. *80:* 7–18.

Wenthold, R. J., D. Huie, R. A. Altschuler, and K. A. Reeks (1987) Glycine immunoreactivity localized in the cochlear nucleus and superior olivary complex. Neuroscience *22:* 897–912.

White, J. S. (1983) Fine structure of the lateral superior olivary nucleus in the albino rat. Soc. Neurosci. Abstr. *9:* 765.

White, J. S. (1984) Fine structural features of medial olivocochlear neurons in the rat. Soc. Neurosci. Abstr. *10:* 393.

White, J. S. (1986) Differences in the ultrastructure of labyrinthine efferent neurons in the albino rat. Assoc. Res. Otolaryngol. Abstr. *9:* 34–35.

White, J. S., and W. B. Warr (1983) The dual origins of the olivocochlear bundle in the albino rat. J. Comp. Neurol. *219:* 203–214.

White, J. S., D. Robertson, and W. B. Warr (1986) Electron-microscopic observations on an HRP-filled, physiologically-characterized medial olivocochlear neuron in the guinea pig cochlea. Soc. Neurosci. Abstr. *12:* 1264.

Woolf, N. K., and A. F. Ryan (1985) Functional ontogeny of neural discharge patterns in the ventral cochlear nucleus of the Mongolian gerbil. Brain Res. *17:* 131–147.